J|A|C|S ARTICLES

Published on Web 02/05/2010

Kinetic and Thermodynamic Analysis of Processes Relevant to Initiation of Olefin Metathesis by Ruthenium Phosphonium Alkylidene Catalysts

Erin M. Leitao,[†] Edwin F. van der Eide,[†] Patricio E. Romero,[†] Warren, E. Piers,[†,*] and Robert McDonald[‡]

Department of Chemistry, University of Calgary, 2500 University Drive NW, Calgary, Alberta, Canada T2N 1N4, and Department of Chemistry, University of Alberta, 11227 Saskatchewan Drive, Edmonton, Alberta, Canada T6G 2G2

Received November 30, 2009; E-mail: wpiers@ucalgary.ca

Abstract: Initiation processes in a family of ruthenium phosphonium alkylidene catalysts, some of which are commercially available, are presented. Seven 16-electron zwitterionic catalyst precursors of general formula $(H_2IMes)(Cl)_3Ru{=}C(H)P(R^1)_2R^2$ ($R^1 = R^2 = C_6H_{11}$, C_5H_9, *i*-C_3H_7, **1-Cy$_3$-Cl**, **1-Cyp$_3$-Cl**, **1-^{i}Pr$_3$-Cl**; $R^1 = C_6H_{11}$, $R^2 = CH_2CH_3$, **1-EtCy$_2$-Cl**; $R^1 = C_6H_{11}$, $R^2 = CH_3$, **1-MeCy$_2$-Cl**; $R^1 =$ *i*-C_3H_7, $R^2 = CH_2CH_3$, **1-Et^{i}Pr$_2$-Cl**; $R^1 =$ *i*-C_3H_7, $R^2 = CH_3$, **1-Me^{i}Pr$_2$-Cl**) were prepared. These compounds can be converted to the metathesis active 14-electron phosphonium alkylidenes by chloride abstraction with $B(C_6F_5)_3$. The examples with symmetrically substituted phosphonium groups exist as monomers in solution and are rapid initiators of olefin metathesis reactions. The unsymmetrically substituted phosphonium alkylidenes are observed to undergo reversible dimerization, the extent of which is dependent on the steric bulk of the phosphonium group. Kinetic and thermodynamic parameters of these equilibria are presented, as well as experiments that show that metathesis is only initiated through the monomers; thus dedimerization is required for initiation. In another detailed study, the series of catalysts **1-R$_3$** were reacted with *o*-isopropoxystyrene under pseudo-first-order conditions to quantify second-order olefin binding rates. A more complex initiation process was observed in that the rates were accelerated by catalytic amounts of ethylene produced in the reaction with *o*-isopropoxystyrene. The ability of the catalyst to generate ethylene is related to the nature of the phosphonium group, and initiation rates can be dramatically increased by the intentional addition of a catalytic amount of ethylene.

Introduction

The development of highly active, selective catalysts for olefin metathesis has been one of the most intense areas of research in modern organometallic chemistry,[1−8] and the accomplishments in the field have been recognized with the highest of accolades.[9−11] A variety of catalyst families are now commercially available, offering many choices to the synthetic chemist, depending on the application and desired characteristics of the catalyst.[12−16] One variable whose manipulation is advantageous is the rate of initiation. Molybdenum-based catalysts are typically very active and rapidly initiating, the process consisting of a bimolecular reaction between the catalyst and an olefin substrate.[5,17−19] However, for the generally more functional group versatile ruthenium-based catalysts, the initiation process consists of a (slower) ligand dissociation step that opens a coordination site for the olefin reactant.[20]

Control of this process is crucial for many olefin metathesis applications, and the ability to slow or speed up the rate of initiation has important consequences for applications in materials synthesis and the range of reaction conditions available. For example, slow initiating catalysts or latent catalysts wherein

[†] University of Calgary.
[‡] University of Alberta.

(1) Schrock, R. R. *Angew. Chem., Int. Ed.* **2006**, *45*, 3748–3759.
(2) Grela, K.; Michrowska, A.; Bieniek, M. *Chem. Rec.* **2006**, *6*, 144–156.
(3) Grubbs, R. H. *Tetrahedron* **2004**, *60*, 7117–7140.
(4) Trnka, T. M.; Grubbs, R. H. *Acc. Chem. Res.* **2001**, *34*, 18–29.
(5) Schrock, R. R.; Hoveyda, A. H. *Angew. Chem., Int. Ed.* **2003**, *42*, 4592–4633.
(6) Mol, J. C. *J. Mol. Catal.* **2004**, *213*, 39–45.
(7) Hoveyda, A. H.; Zhugralin, A. R. *Nature* **2007**, *450*, 243–251.
(8) Nicolau, K. C. B., P. G.; Sariah, D. *Angew. Chem., Int. Ed.* **2005**, *44*, 4490–4527.
(9) Chauvin, Y. *Angew. Chem., Int. Ed.* **2006**, *45*, 3740–3747.
(10) Schrock, R. R. *Angew. Chem., Int. Ed.* **2006**, *45*, 3748–3759.
(11) Grubbs, R. H. *Angew. Chem., Int. Ed.* **2006**, *45*, 3760–3765.
(12) Blanc, F.; Thivolle-Cazat, J.; Basset, J.-M.; Copéret, C.; Hock, A. S.; Tonzetich, Z. J.; Sinha, A.; Schrock, R. R. *J. Am. Chem. Soc.* **2007**, *129*, 1044–1045.
(13) Schwab, P.; France, M. B.; Ziller, J. W.; Grubbs, R. H. *Angew. Chem., Int. Ed.* **1995**, *34*, 2039–2041.
(14) Schwab, P.; Grubbs, R. H.; Ziller, J. W. *J. Am. Chem. Soc.* **1996**, *118*, 100–110.
(15) Michrowska, A.; Grela, K. *Pure Appl. Chem.* **2008**, *80*, 31–43.
(16) Bieniek, M.; Michrowska, A.; Usanov, D. L.; Grela, K. *Chem. Eur. J.* **2008**, *14*, 806–818.
(17) ThornCsanyi, E.; Dehmel, J.; Luginsland, H. D.; Zilles, J. U. *J. Mol. Catal.* **1997**, *115*, 29–35.
(18) Bailey, B. C.; Schrock, R. R.; Kundu, S.; Goldman, A. S.; Huang, Z.; Brookhart, M. *Organometallics* **2009**, *28*, 355–360.
(19) Cortez, G. A.; Baxter, C. A.; Schrock, R. R.; Hoveyda, A. H. *Org. Lett.* **2007**, *9*, 2871–2874.
(20) Sanford, M. S.; Love, J. A.; Grubbs, R. H. *J. Am. Chem. Soc.* **2001**, *123*, 6543–6554.

10.1021/ja910112m

Chart 1

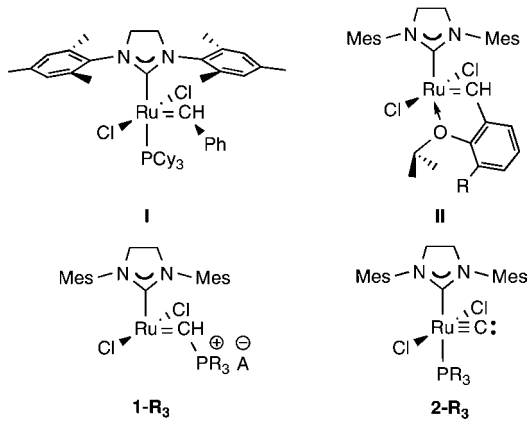

initiation can be triggered by some external stimulus are important in ROMP applications where physical manipulation of the catalyst within the monomer prior to polymerization is advantageous.[21−27] On the other hand, fast initiating catalysts[28] are advantageous for ROMP applications where more monodisperse polymers are desired. Furthermore, rapidly initiating catalysts[29] allow for other metathesis reactions (such as cross metathesis or asymmetric ring closing metathesis) to be run at much lower temperatures, leading to increased selectivity.

Development of fast initiating catalysts in ruthenium-based, Grubbs-type catalysts has focused on lowering the barrier to dissociation of a ligand L to generate the active 14-electron alkylidene complexes shown to be the active species.[20,30] Strategies have therefore included replacing the PCy_3 ligand of the Grubbs generation 2 catalyst, **I** (Chart 1), with weakly basic ligands such as *m*-bromopyridine[28,31] or increasing the steric bulk of the hemilabile portion of the alkylidene ligand in the Grubbs−Hoveyda family of catalysts, **II**,[32,33] through manipulation of R.[34−36] Both strategies result in more rapid dissociation of the ligand, increasing the initiation rates relative to the parent system.

Another strategy for lowering the initiation barrier is to remove the ligand that needs to dissociate altogether, rendering the initiation step more akin to that in the molybdenum-based systems. We serendipitously discovered a way to do this by preparing the family of 14-electron phosphonium alkylidenes **1-R$_3$** via protonation of the ruthenium carbides **2-R$_3$**.[29] This apparently triggers a migration of the phosphine ligand to the protonated carbide carbon, leaving a vacant coordination site and sequestering the phosphine in the vinylphosphonium salt eliminated upon the first metathesis event.[37,38] Qualitatively, these catalysts are among the fastest initiating species known and are highly active even at low temperatures, rivaling the performance of the early metal catalysts while retaining the functional group tolerance and versatility associated with the ruthenium-based family of catalysts.

Presumably, initiation in these catalysts involves bimolecular coordination of substrate rather than unimolecular ligand dissociation as in conventional ruthenium-based catalyst systems.[20,30] Another potential issue is the orientation of the phosphonium alkylidene ligand, which in the ground state of compound **1-Cy$_3$** is perpendicular to the correct orientation for ruthenacyclobutane formation upon reaction with an olefin substrate.[29,39] Herein we explore the nature of the initiation process in the 14-electron phosphonium alkylidene catalysts **1-R$_3$** and examine the effect of changing the phosphine substituents R on these processes.[40] Although it is clear that the nature of R plays a significant role in determining the initiation rate,[41] these studies reveal a complex network of initiation chemistry in which dimerization/dedimerization and the generation of catalytic amounts of ethylene are important issues.

Results and Discussion

Synthesis. In order to examine initiation processes in phosphonium alkylidene catalysts **1**, synthetic routes to a variety of catalysts differing in the alkyl substituents on phosphorus were required. The original synthesis of **1-Cy$_3$** involved protonation of the corresponding carbide **2-Cy$_3$** with a variety of acids; therefore, to broaden the range of phosphorus substituents, several new carbide complexes were required. In 2001 Sanford et al. showed that the six-coordinate bis(pyridine) complex $(H_2IMes)(Cl)_2(py)_2Ru{=}C(H)Ph$ is an excellent synthon for the preparation of ruthenium benzylidenes with a wide variety of phosphines.[20] Reaction with 1.1 equiv of a phosphine produced the desired benzylidene, which could be isolated in good yields after a simple workup. This is how we synthesized the Grubbs generation 2 catalyst analogues **I-Cyp$_3$** and **I-^{i}Pr$_3$**, using the symmetrical trialkylphosphines tricyclopentylphosphine (cone angle = 167°) and triisopropylphosphines (160°), respectively.[42] For the unsymmetrically substituted phosphines $PMeCy_2$, PMe^iPr_2, $PEtCy_2$, and PEt^iPr_2, which are not commercially available, the new methodology outlined in Scheme 1 allowed

(21) P'Pool, S. J.; Schanz, H.-J. *J. Am. Chem. Soc.* **2007**, *129*, 14200–14212.
(22) Diesendruck, C. E.; Vidavsky, Y.; Ben-Asuly, A.; Lemcoff, N. G. *J. Polym. Sci. Part A: Polym. Chem.* **2009**, *47*, 4209–4213.
(23) Balof, S. L.; Yu, B.; Lowe, A. B.; Ling, Y.; Zhang, Y.; Schanz, H. J. *Eur. J. Inorg. Chem.* **2009**, 1717–1722.
(24) Hejl, A.; Day, M. W.; Grubbs, R. H. *Organometallics* **2006**, *25*, 6149–6154.
(25) Ung, T.; Hejl, A.; Grubbs, R. H.; Schrodi, Y. *Organometallics* **2004**, *23*, 5399–5401.
(26) Monsaert, S.; Drozdzak, R.; Verpoort, F. *Chim. Oggi* **2008**, *26*, 93.
(27) Piermattei, A.; Karthikeyan, S.; Sijbesma, R. P. *Nat. Chem.* **2009**, *1*, 133–137.
(28) Sanford, M. S.; Love, J. A.; Grubbs, R. H. *Organometallics* **2001**, *20*, 5314–5318.
(29) Romero, P. E.; Piers, W. E.; McDonald, R. *Angew. Chem., Int. Ed.* **2004**, *43*, 6161–6165.
(30) Dias, E. L.; Nguyen, S. T.; Grubbs, R. H. *J. Am. Chem. Soc.* **1997**, *119*, 3887–3897.
(31) Love, J. A.; Morgan, J. P.; Trnka, T. M.; Grubbs, R. H. *Angew. Chem., Int. Ed.* **2002**, *41*, 4035–4037.
(32) Kingsbury, J. S.; Harrity, J. P. A.; Bonitatebus, P. J.; Hoveyda, A. H. *J. Am. Chem. Soc.* **1999**, *121*, 791–799.
(33) Garber, S. B.; Kingsbury, J. S.; Gray, B. L.; Hoveyda, A. H. *J. Am. Chem. Soc.* **2000**, *122*, 8168–8179.
(34) Wakamatsu, H.; Blechert, S. *Angew. Chem., Int. Ed.* **2002**, *41*, 794–796.
(35) Wakamatsu, H.; Blechert, S. *Angew. Chem., Int. Ed.* **2002**, *41*, 2403–2405.
(36) Bujok, R.; Bieniek, M.; Masnyk, M.; Michrowska, A.; Sarosiek, A.; Stepowska, H.; Arlt, D.; Grela, K. *J. Org. Chem.* **2004**, *69*, 6894–6896.
(37) Romero, P. E. 14-Electron Phosphonium Alkylidenes in Olefin Metathesis: A Synthetic and Mechanistic Study. Ph.D. Dissertation, University of Calgary, 2006.
(38) Macnaughtan, M. L.; Johnson, M. J. A.; Kampf, J. W. *J. Am. Chem. Soc.* **2007**, *129*, 7708–7709.
(39) Romero, P. E.; Piers, W. E. *J. Am. Chem. Soc.* **2005**, *127*, 5032–5033.
(40) Li, C. B.; Ogasawara, M.; Nolan, S. P.; Caulton, K. G. *Organometallics* **1996**, *15*, 4900–4903.
(41) Love, J. A.; Sanford, M. S.; Day, M. W.; Grubbs, R. H. *J. Am. Chem. Soc.* **2003**, *125*, 10103–10109.
(42) Tolman, C. A. *Chem. Rev.* **1977**, *77*, 313–348.

Scheme 1

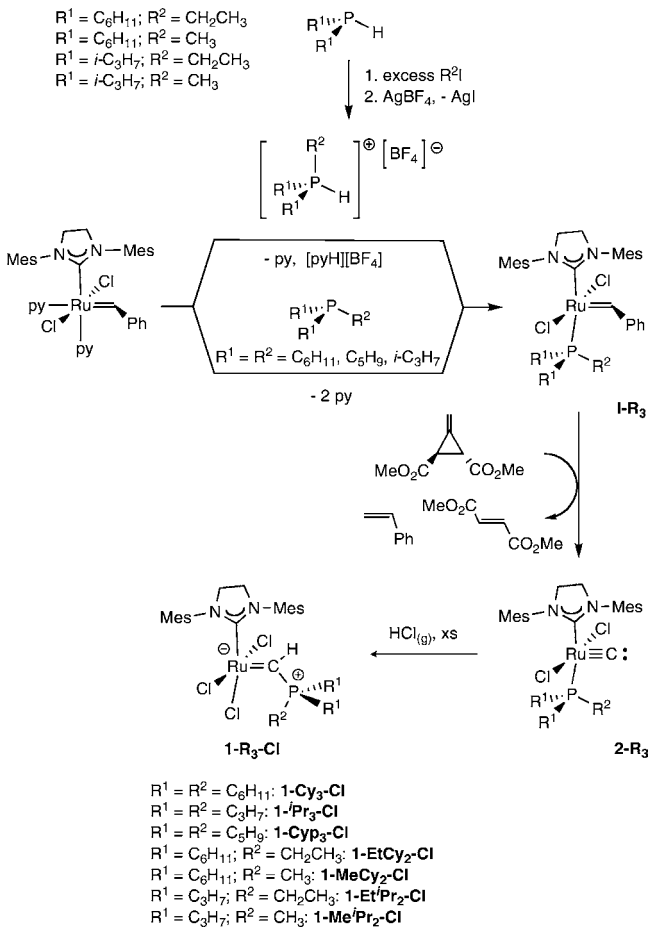

for the convenient introduction of these phosphines through their air-stable phosphonium salts. While the reactions of $HP(R^1)_2$ (R^1 = Cy, ^{i}Pr) with an excess of methyl or ethyl iodide in ether/hexane proceeded with variable rates, the reactions cleanly yielded $[HP(R^1)_2R^2]I$ as white precipitates if given enough time (Scheme 1). The iodide salts were then treated with $AgBF_4$ to form the corresponding tetrafluoroborate salts, to avoid partial incorporation of iodide[20,30] into the ruthenium benzylidene chlorides **I-R$_3$** in the subsequent reaction. All of the hydrophosphonium salts are air-stable and can be worked up and isolated on the benchtop. Their ^{1}H NMR spectra show a doublet of multiplets for the phosphorus-bound proton with $^1J_{HP}$ of ca. 480 Hz, typical values for tertiary phosphonium cations.[43,44]

The reaction of $(H_2IMes)(Cl)_2(py)_2Ru{=}C(H)Ph$ with 1.1 equiv of $[HP(R^1)_2R^2][BF_4]$ readily proceeded in toluene to form $P(R^1)_2R^2$-ligated benzylidenes **I-R$_3$**, with loss of 1 equiv of pyridine and $[pyH][BF_4]$ precipitating as a byproduct. In these reactions, it is plausible that a dissociated pyridine first deprotonates the phosphonium cation to form the phosphine in situ; then the phosphine coordinates to the ruthenium to form compounds **I**. Indeed, ^{1}H and ^{31}P NMR spectra corresponding to free $PMeCy_2$ were obtained in pyridine-d_5 solutions of $[HP(Me)Cy_2]I$, and deprotonation of related phosphonium cations with triethylamine is a known method to prepare phosphines.[43,44] The benzylidenes **I-R$_3$**, some of which are new derivatives of the Grubbs generation 2 catalyst family, were obtained analytically pure after passage through a plug of silica, in isolated yields of 80−90%. Their ^{1}H NMR spectra show a diagnostic sharp singlet at ca. 19 ppm for the benzylidene proton; further details can be found in Supporting Information.

The benzylidenes **I-R$_3$** were then converted into the carbide complexes **2-R$_3$** by the Heppert methodology using Feist's ester.[45] In order to obtain good yields of the $PMeCy_2$ and PMe^iPr_2 derivatives, it was necessary to heat the reaction mixtures to 45 °C for ca. 16 h. Presumably, the decreased steric bulk of the methyl-substituted phosphines (relative to PCy_3, $PCyp_3$, and P^iPr_3) results in a decrease in the rate of metathesis with Feist's ester, which is likely the rate-limiting step in carbide formation, in this case.[46] Carbides were obtained analytically pure in yields of 60−80% after passage over a plug of silica. A diagnostic feature in their ^{13}C NMR spectra is the signal for Ru≡*C* at ca. 480 ppm, which is always observed as a singlet (i.e., no discernible $^2J_{CP}$). The H_2IMes carbene carbons resonate at ca. 212 ppm, with $^2J_{CP}$ ca. 85 Hz; complete spectroscopic and synthetic details are given in Supporting Information.

Protonation of the carbides **2-R$_3$** converts them into phosphonium alkylidenes **1-R$_3$**. When acids with weakly coordinating anions (e.g., $[B(C_6F_5)_4]^-$, or OTf^-)[47] are employed, significant amounts of $[H_2IMesH]^+$ are observed for the less bulky phosphines, indicating emergent competitive protonation of the NHC carbene as the steric bulk of the phosphine decreases. Furthermore, the decomposition rates of the four-coordinate phosphonium alkylidenes with less bulky groups on phosphorus are faster, hampering isolation of pure compounds.[48] These problems were avoided by preparing the air-stable, zwitterionic trichlorides **1-R$_3$-Cl** via protonation of the carbides with an excess of gaseous HCl in dichloromethane. Macnaughtan et al.[49] showed that, for the carbide **2-PCy$_3$**, this reaction proceeds through the red chloromethylidene intermediate $(H_2IMes)(Cl)_2(PCy_3)Ru{=}C(H)Cl$, which rearranges to **1-Cy$_3$-Cl** at room temperature. We presume that analogous intermediates are formed in all of the reactions, as introduction of HCl into the reaction flask at −78 °C always resulted in a color change from light yellow (carbide) to red; in addition, we observed the intermediate by NMR spectroscopy for the $MePR_2$ derivatives. For the PCy_3, $PCyp_3$, P^iPr_3, $PEtCy_2$, and PEt^iPr_2 derivatives, the red color fades within 2 h at room temperature to cleanly give yellow/green solutions of **1-R$_3$-Cl**. The red color persists for the $PMeCy_2$ and PMe^iPr_2 derivatives; a 15 h reaction time was found to be optimal for these derivatives. All of the trichlorides were purified by crystallization to obtain analytically pure materials, typically in 80% yield; the yield is 50−60% for **1-MeCy$_2$-Cl** and **1-Me^{i}Pr$_2$-Cl**, because during the required prolonged reaction times they slowly react with HCl to form other products.[50] Five-coordinate trichlorides **1-R$_3$-Cl** have C_s

(43) Goerlich, J. R.; Schmutzler, R. *Phosphorus, Sulfur Silicon Relat. Elem.* **1993**, *81*, 141–148.
(44) Tewari, A.; Hein, M.; Zapf, A.; Beller, M. *Synthesis* **2004**, 935–941.
(45) Carlson, R. G.; Gile, M. A.; Heppert, J. A.; Mason, M. H.; Powell, D. R.; Vander Velde, D.; Vilain, J. M. *J. Am. Chem. Soc.* **2002**, *124*, 1580–1581.
(46) Hejl, A.; Trnka, T. M.; Day, M. W.; Grubbs, R. H. *Chem. Commun.* **2002**, 2524–2525.
(47) Jutzi, P.; Müller, C.; Stammler, A.; Stammler, H.-G. *Organometallics* **2000**, *19*, 1442–1444.
(48) Leitao, E. M.; Dubberley, S. R.; Piers, W. E.; Wu, Q.; McDonald, R. *Chem. Eur. J.* **2008**, *14*, 11565–11572.
(49) Macnaughtan, M. L.; Johnson, M. J. A.; Kampf, J. W. *Organometallics* **2007**, *26*, 780–782.
(50) One of these by-products is the red, paramagnetic phosphonium alkyl $(H_2IMes)(Cl)_3RuCH_2P(Me)R_2$ analyzed by X-ray diffraction for R = Cy. The mechanism for the formation of this byproduct remains unknown.

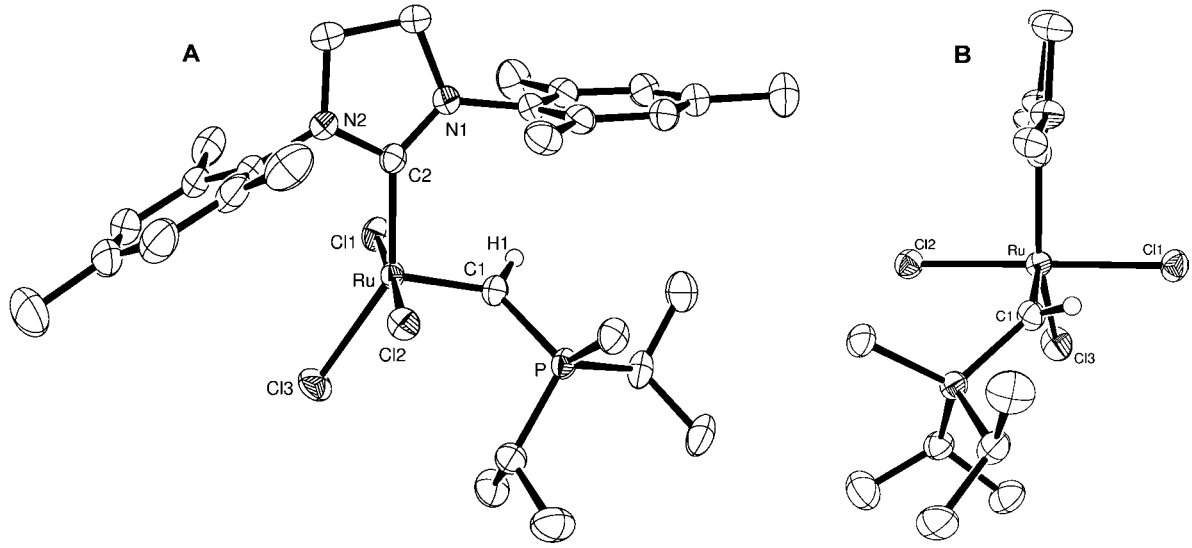

Figure 1. Crystal structure of **1-Me^{i}Pr$_2$-Cl**: (A) front view; (B) side view. See Supporting Information for an ORTEP diagram of **1-MeCy$_2$-Cl**

Table 1. Selected Metrical Parameters for **1-Me^{i}Pr$_2$-Cl** and **1-MeCy$_2$-Cl**

parameter[a]	**1-MeCy$_2$-Cl** · 3CHCl$_3$	**1-Me^{i}Pr$_2$-Cl** · 1.5CH$_2$Cl$_2$
Ru−C1	1.823(3)	1.818(3)
Ru−C2	2.022(3)	2.022(3)
Ru−Cl3	2.3553(9)	2.3465(9)
Ru−Cl2	2.3699(8)	2.3777(8)
Ru−Cl1	2.4002(8)	2.4034(8)
C1−P	1.806(3)	1.814(3)
C2−Ru−Cl3	145.97(9)	145.98(9)
Cl1−Ru−Cl2	176.50(3)	176.94(3)
C1−Ru−C2	100.48(13)	101.55(13)
Ru−C1−P	127.46(19)	127.16(18)
C2−Ru−C1−P	125.4(2)	121.7(2)

[a] Distances in Å, angles and dihedrals in deg.

symmetry in solution and display a characteristic doublet at 19.3−19.7 ppm in the ^{1}H NMR spectra, with $^2J_{HP}$ of 50−54 Hz for the alkylidene proton. These shifts and coupling constants were quite distinct from those of four-coordinate complexes (δ ∼17.8 ppm, $^2J_{HP}$ ∼35 Hz), and indeed, these parameters are a useful diagnostic for assaying the coordination environment about ruthenium (*vide infra*). Compared to the carbides, the **1-R$_3$-Cl** H$_2$IMes carbene carbons were at very similar chemical shifts of ca. 212 ppm, but with $^3J_{CP}$ ∼3 Hz that are significantly smaller (cf. $^2J_{CP}$ ∼85 Hz for carbides).

The structures of **1-Cy$_3$-Cl** and **1-^{i}Pr$_3$-Cl** have been published elsewhere.[49,51] In these, the dihedral angles, C_{NHC}−Ru−C−P, are 150° or larger in order to avoid unfavorable steric interactions between the Cy/^{i}Pr and Mes groups of the NHC and fixing the phosphonium alkylidene in an orientation approximately perpendicular to that necessary for [2 + 2] cycloaddition with an olefin in the first metathesis event. In **1-MeCy$_2$-Cl** and **1-Me^{i}Pr$_2$-Cl** (Figure 1, only **1-Me^{i}Pr$_2$-Cl** displayed), the smaller methyl substituents allow for a more pronounced rotation around the Ru=C bond, and the C_{NHC}−Ru−C−P dihedrals become 125.4(2)° and 121.7(2)°, respectively (Table 1). As a result of the rotation of the ruthenium-carbon π bond out of the C1−Ru−Cl1−Cl2 plane and into the C1−Ru−C2−Cl3 plane, the Cl1−Ru−Cl2 angles open up to ∼177° and the C2−Ru−Cl3 angles contract to ∼146°. Additionally, although Cl3 is positioned trans to the strong σ-donor H$_2$IMes, the Ru-Cl3 bond is shorter than the other two Ru-Cl bonds. This stands in contrast to the structure of **1-^{i}Pr$_3$-Cl**, in which the Ru-Cl bond trans to H$_2$IMes is 0.13 Å longer than the other Ru-Cl bonds.[51] The geometry around Ru can be described as trigonal bipyramidal, with Cl1 and Cl2 occupying the apexes and C1, C2, and Cl3 forming a quite distorted trigonal plane. These structures suggest that an electronic preference may exist for the perpendicular orientation of the alkylidene unit relative to the C2−Ru−Cl3 plane. However, a larger sampling of complexes **1-R$_3$-Cl**, with phosphines smaller than PMe^{i}Pr$_2$, is necessary to make definite conclusions. It should also be noted that, despite the observed dissymmetry in the solid state, ^{1}H NMR spectra of **1-MeCy$_2$-Cl** and **1-Me^{i}Pr$_2$-Cl** indicate C_s symmetry at all accessible (low) temperatures, implying that the barrier to Ru=C bond rotation is low in solution.

Scheme 2

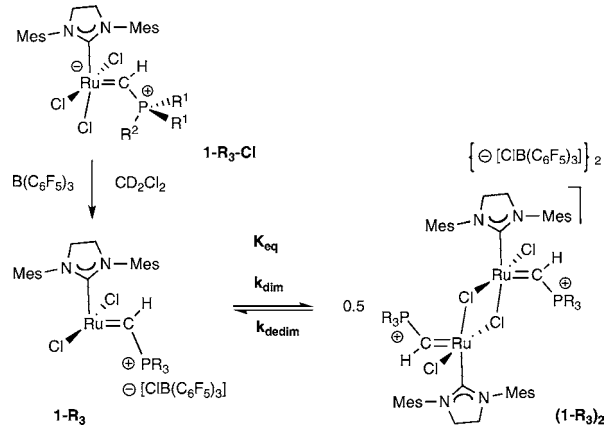

Trichlorides **1-R$_3$-Cl** do not mediate olefin metathesis reaction but may be activated via chloride abstraction with B(C$_6$F$_5$)$_3$ in dichloromethane (Scheme 2). Admixture of these two components rapidly and quantitatively generates 14-electron cationic complexes **1-R$_3$**. BCl$_3$ and ClB(C$_6$F$_5$)$_2$ were also found to be capable chloride abstraction agents, but B(C$_6$F$_5$)$_3$ was used because of its ease of handling. Phosphonium alkylidenes **1-Cy$_3$**, **1-Cyp$_3$**, and **1-^{i}Pr$_3$** are each strictly monomeric at all accessible

(51) van der Eide, E. F.; Romero, P. E.; Piers, W. E. *J. Am. Chem. Soc.* **2008**, *130*, 4485–4491.

temperatures, as judged from the observation of only one Ru=C(*H*)P doublet in the ^{1}H NMR spectra at δ ~17.8 ppm with $^2J_{HP}$ ~35 Hz throughout the temperature range 300−190 K. Additionally, ^{1}H and ^{31}P NMR resonances pertaining to the Ru fragment are indistinguishable between the $ClB(C_6F_5)_3$ and the $B(C_6F_5)_4$ salts, indicating that the chloroborate counteranion is essentially noncoordinating toward the ruthenium in these ion pairs.

In contrast, the mixed-alkyl derivatives **1-MeCy$_2$**, **1-Me^{i}Pr$_2$**, **1-EtCy$_2$**, and **1-Et^{i}Pr$_2$** have a tendency to reversibly dimerize in solution to form centrosymmetric dimers **(1-R$_3$)$_2$** (Scheme 2), the extent of dimerization depending on the size of the P substituents. It is likely that the small alkyl group allows the phosphonium alkylidene to rotate toward the mesityl (as seen in the crystal structures of **1-Me^{i}Pr$_2$-Cl** and **1-MeCy$_2$-Cl**), which makes the ruthenium centers accessible for dimerization. In the ^{1}H NMR spectra, the dimers are characterized by a doublet at δ ~19.5 ppm with $^2J_{HP}$ ~46 Hz for the alkylidene proton. The similarity of the chemical shift and proton-phosphorus coupling constant to those of the trichlorides (δ ~19.5 ppm, $^2J_{HP}$ ~52 Hz) is a strong argument for the five-coordinate nature of ruthenium in the dimeric structures. The ^{1}H and ^{13}C NMR spectra further indicate that the dimers have C_i symmetry, and on the basis of these data we assign the structures as shown in Scheme 2, with the ruthenium centers bridged by two chlorides, thus giving both metal centers a 16-electron configuration and rendering them five-coordinate. Despite many attempts, we have not been able to obtain single crystals of any such dimer, but we note that Johnson et al. have crystallographically characterized a neutral dimer of this general structure incorporating =C(F)H groups instead of phosphonium alkylidenes as in **(1-R$_3$)$_2$**.[52] In addition, Hofmann and co-workers have observed dimeric, dicationic complexes of the type $\{[(PP)Ru{=}C(H)R]_2(\mu\text{-}Cl)_2\}^{2+}$ (R = C(H)=C(Me)$_2$, ^{i}Pr; PP = ^{t}Bu$_2$PCH$_2$P^{t}Bu$_2$, ^{t}Bu$_2$PCH$_2$CH$_2$P^{t}Bu$_2$) containing triflate anions that undergo cis−trans interconversion in solution.[53,54] Astruc and co-workers have also observed related dicationic dimers.[55]

Dimerization/Dedimerizaton Equilibria. The observation of dimerization is significant given the role that dimerization has been proposed to play in the deactivation of ruthenium-based olefin metathesis catalysts. For example, other ruthenium-based olefin metathesis catalysts have demonstrated the tendency to dimerize especially when heated,[56,57] during decomposition,[58,48] or in the presence of certain substrates.[52] Grubbs and co-workers found that the methylidene catalyst decomposes at 328 K in benzene to give a dinuclear ruthenium compound with a bridging carbide between the two ruthenium centers, where one of the metal centers contains a hydride ligand, leaving a methyl phosphonium salt byproduct.[56] Fogg et al. and our group both found that decomposition of ruthenium catalysts containing chloride ligands formed chloride-bridged dimers.[48,53] Since this discovery, Fogg and co-workers have produced catalysts

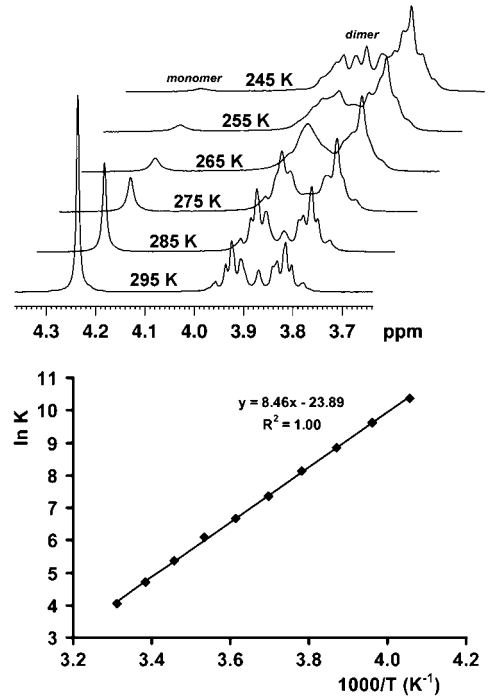

Figure 2. Stacked fragments of variable temperature ^{1}H NMR spectra (top) and van't Hoff plot (bottom) for the equilibrium of **1-MeCy$_2$** with **(1-MeCy$_2$)$_2$**.

incapable of dimerizing in the same manner by replacing the chlorides with aryloxides ("pseudohalide") ligands.[59−63] Finally, in the presence of excess monohalogenated olefins (chloride, fluoride), the Hoveyda catalyst **II** reacts to form a centrosymmetric dimer containing the monohalogenated carbene.[52] Furthermore, since the dimerization of the phosphonium alkylidenes **1** is likely to impact the rates of reaction with olefin substrates significantly, i.e., the rate of initiation for this family of catalysts, we embarked on a detailed analysis of the thermodynamic and kinetic (vide infra) aspects of these monomer−dimer equilibria.

A van't Hoff plot for the monomer−dimer equilibrium of **1-MeCy$_2$** (Figure 2) in the temperature range of 245−295 K gives $\Delta H° = -70(2)$ kJ mol^{-1} and $\Delta S° = -199(10)$ J mol^{-1} K^{-1}. The ^{1}H NMR signals for the H_2IMes NCH_2CH_2N backbone (Figure 2) were used in this analysis, since they are distinct and do not overlap with each other or with other peaks. The dimer shows an AA′BB′ pattern for these protons at room temperature, due to fast rotation around the C_{NHC}−Ru bond. This transforms into an ABCD pattern as the temperature is lowered, and the rotation is slowed, rendering all four protons chemically inequivalent. The monomer−dimer character of the equilibrium observed is clearly supported by the large negative reaction entropy. In addition, we find that the monomer−dimer ratio depends on the total ruthenium concentration, with higher concentrations shifting the equilibrium toward the dimer. A van't Hoff analysis for slightly bulkier derivative **1-EtCy$_2$** in the temperature range 225−260 K gave $\Delta H = -49(2)$ kJ mol^{-1}

(52) Macnaughtan, M. L.; Gary, J. B.; Gerlach, D. L.; Johnson, M. J. A.; Kampf, J. W. *Organometallics* **2009**, *28*, 2880–2887.
(53) Volland, M. A. O.; Hansen, S. M.; Rominger, F.; Hofmann, P. *Organometallics* **2004**, *23*, 800–816.
(54) Hansen, S. M.; Volland, M. A. O.; Rominger, F.; Eisenträger, F.; Hofmann, P. *Angew. Chem., Int. Ed.* **1999**, *38*, 1273–1276.
(55) Gatard, S.; Kahlal, S.; Mery, D.; Nlate, S.; Cloutet, E.; Saillard, J. Y.; Astruc, D. *Organometallics* **2004**, *23*, 1313–1324.
(56) Hong, S. H.; Wenzel, A. G.; Salguero, T. T.; Day, M. W.; Grubbs, R. H. *J. Am. Chem. Soc.* **2007**, *129*, 7961–7968.
(57) Hong, S. H.; Day, M. W.; Grubbs, R. H. *J. Am. Chem. Soc.* **2004**, *126*, 7414–7415.
(58) Conrad, J. C.; Fogg, D. E. *Curr. Org. Chem.* **2006**, *10*, 185–202.
(59) Conrad, J. C.; Camm, K. D.; Fogg, D. E. *Inorg. Chim. Acta* **2006**, *359*, 1967–1973.
(60) Conrad, J. C.; Amoroso, D.; Czechura, P.; Yap, G. P. A.; Fogg, D. E. *Organometallics* **2003**, *22*, 3634–3636.
(61) Conrad, J. C.; Parnas, H. H.; Snelgrove, J. L.; Fogg, D. E. *J. Am. Chem. Soc.* **2005**, *127*, 11882–11883.
(62) Drouin, S. D.; Foucault, H. M.; Yap, G. P. A.; Fogg, D. E. *Can. J. Chem.* **2005**, *83*, 748–754.
(63) Monfette, S.; Fogg, D. E. *Organometallics* **2006**, *25*, 1940–1944.

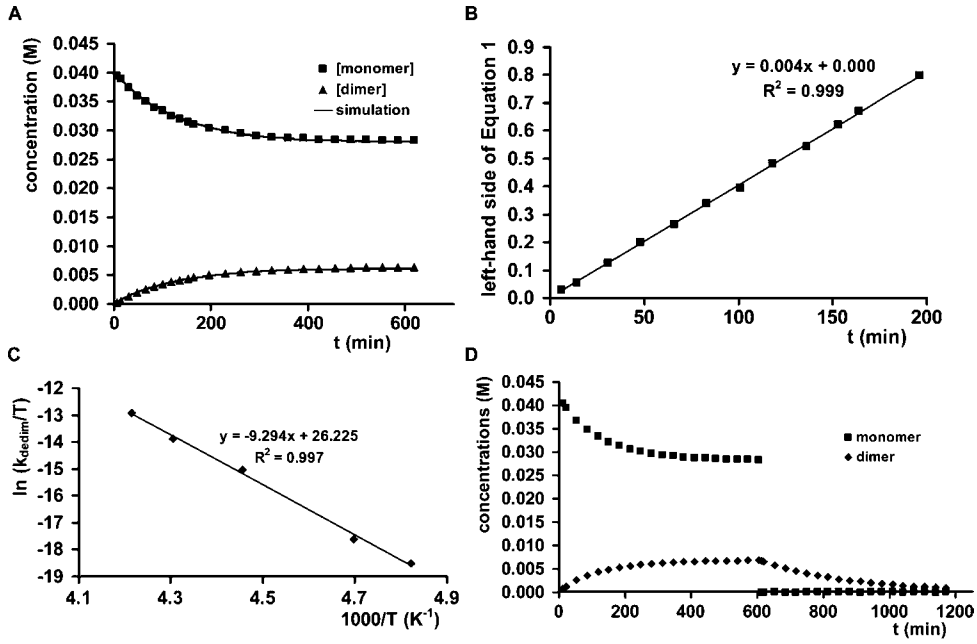

Figure 3. (A) Equilibration of **1-EtCy$_2$** with **(1-EtCy$_2$)$_2$** at 225 K and simulation of reaction profile. (B) Determination of k_{dedim} by logarithmic plot using eq 1. (C) Eyring plot for the dedimerization of **(1-EtCy$_2$)$_2$**. (D) Equilibration of **1-EtCy$_2$** with **(1-EtCy$_2$)$_2$** at 225 K, followed by addition of excess ethylene at $t = 600$ min.

and $\Delta S = -198(10)$ J mol^{-1} K^{-1}. Notably, the reaction entropy is the same as observed for **1-MeCy$_2$**, but the reaction enthalpy is decidedly less negative than the $-70(2)$ kJ mol^{-1} found for **1-MeCy$_2$**. The increased steric bulk of **1-EtCy$_2$** relative to **1-MeCy$_2$** presumably results in an enthalpic stabilization of the monomeric form, a destabilization of the dimeric form, or a combination of these effects.

The four mixed-phosphine species (**1-Me^{i}Pr$_2$**, **1-MeCy$_2$**, **1-Et^{i}Pr$_2$**, **1-EtCy$_2$**) show a similar tendency to dimerize; however, the temperature range where, by NMR, there is observable monomer in equilibrium with dimer for each of the catalysts varies significantly. The smaller catalysts (**1-Me^{i}Pr$_2$**, **1-MeCy$_2$**) are mostly dimer at room temperature and increasing the temperature favors dimer dissociation, whereas increasing the bulk of the phosphine favors monomer at room temperature. We were able to find a temperature where all four catalysts had detectable amounts of monomer and dimer by NMR for comparison. At 272 K, a small amount of monomer was present in the **1-Me^{i}Pr$_2$** catalyst providing an equilibrium constant, K_{eq}, of $1.26(5) \times 10^3$ M^{-1}, followed by **1-MeCy$_2$** catalyst at $6.54(5) \times 10^1$ M^{-1}, **1-Et^{i}Pr$_2$** at $8.07(5) \times 10^{-1}$ M^{-1}, and **1-EtCy$_2$** as mostly monomer at $5.57(5) \times 10^{-3}$ M^{-1}. Thus, subtle changes in the substitution at phosphorus result in a range of almost 6 orders of magnitude in the value of K_{eq}.

The character of the **1-EtCy$_2$/(1-EtCy$_2$)$_2$** equilibrium in particular provided an opportunity to study the kinetics associated with the equilibration, i.e., the extraction of second-order dimerization (k_{dim}) and first-order dedimerization (k_{dedim}) rate constants. **1-EtCy$_2$** exists virtually only in its monomeric form at room temperature (no dimer was detectable by NMR). Signals indicative of the dimer grow in over a period of hours at temperatures of ca. -50 °C, whereas the dimerization is negligibly slow at -78 °C. Thus, fast cooling of room temperature solutions of **1-EtCy$_2$** to -78 °C traps it in its monomeric form. Subsequent insertion into a cooled NMR probe and monitoring the concentrations of **1-EtCy$_2$** and **(1-EtCy$_2$)$_2$** over time affords speciation diagrams like the one displayed in Figure 3A. Assuming that $[\text{dimer}]_0 = 0$ (the line for [dimer] was always found to pass through the origin), eq 1 (see Supporting Information for derivation) gives the integrated rate law that is used to obtain k_{dedim}.[64] The only requirement is that the constants $[\text{monomer}]_0$ and K_{eq} ($= [\text{dimer}]_{eq}/[\text{monomer}]^2_{eq} = k_{dim}/k_{dedim}$) are known. We find that the logarithmic plots are quite linear (see Figure 3B) for the period in which 75% of the total change in concentrations takes place. Data points beyond this time tend to deviate from the line; this is why only the first 200 min are displayed in the linear plot of Figure 3. At 225 K, $k_{dedim} = 6.7(2) \times 10^{-5}$ s^{-1} was thus determined, corresponding to $\Delta G^{\ddagger} = 72.6$ kJ mol^{-1} for dedimerization. From the experimental equilibrium constant $K_{eq} = 8.0(1)$ M^{-1}, $k_{dim} = 5.3(2) \times 10^{-4}$ M^{-1} s^{-1} can be derived, which gives $\Delta G^{\ddagger} = 68.7$ kJ mol^{-1} for dimerization. Using the values for k_{dim} and k_{dedim} in Chemical Kinetics Simulator[65] yielded excellent agreement between observed and simulated reaction profiles (Figure 3A), lending credence to the derived rate constants.

$$k_{dedim}t = \frac{1}{\sqrt{D}} \ln \left| \frac{(4K[\text{monomer}]_0 + 1 - \sqrt{D})(4K[\text{monomer}]_t + 1 + \sqrt{D})}{(4K[\text{monomer}]_0 + 1 + \sqrt{D})(4K[\text{monomer}]_t + 1 - \sqrt{D})} \right| \quad (1)$$

$$D = 1 + 8K[\text{monomer}]_0 \quad (2)$$

The dimerization/dedimerization kinetics were studied in this manner in the temperature range 207−237 K, and an Eyring plot for k_{dedim} is also given in Figure 3C. It should be noted that at the two lowest temperatures, 207 and 213 K, equilibrium was not attained even after 14 h. For these data sets, experi-

(64) Orrell, K. G.; Stephenson, D.; Rault, T. *Magn. Reson. Chem.* **1989**, *27*, 368–376.
(65) Hinsberg, W.; Houle, F.; Allen, F. *Chemical Kinetics Simulator*, *v1.01*; IBM: Almaden Research Center, 1996.

Scheme 3

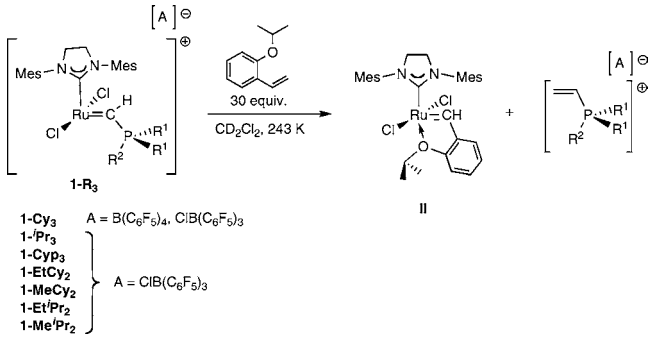

mental K_{eq} values were therefore unavailable; the values extrapolated from the van't Hoff analysis were used. Above 237 K, equilibrium was attained within 30 min and the amount of dimer formed was too small for a reliable kinetic analysis. The Eyring plot yields activation parameters $\Delta H^{\ddagger} = 77(5)$ kJ mol^{-1} and $\Delta S^{\ddagger} = 20(10)$ J mol^{-1} K^{-1}, values consistent with a dedimerization process. (Although the data looks well behaved, given the narrow range of temperatures practically available, the value for $\Delta S^{\ddagger}$ must be interpreted with some caution.)

The impact of the monomer−dimer equilibrium on the ability of this catalyst family to initiate olefin metathesis is illustrated by the reactivity of **1-EtCy$_2$/(1-EtCy$_2$)$_2$** with ethylene. When an excess of ethylene was added to an equilibrated mixture of **1-EtCy$_2$** and **(1-EtCy$_2$)$_2$** at 225 K (Figure 3D), all of the monomer was immediately transformed into the known ruthenacyclobutane $(H_2IMes)(Cl)_2Ru(CH_2)_3$.[66] The dimer concentration then exponentially decreased over time with an observed rate constant (k_{obs}) of 6.3(2) × 10^{-5} s^{-1} which is in very good agreement with k_{dedim} (6.7(2) × 10^{-5} s^{-1}) observed at this temperature. We therefore conclude that ethylene reacts only with monomeric **1-R$_3$** and dimeric **(1-R$_3$)$_2$** does not react with ethylene; the rate-limiting step in its disappearance is dissociation into monomeric **1-R$_3$**. Thus, under conditions where the dimer dominates, initiation of metathesis requires dedimerization in order to proceed.

Initiation Kinetics with *o*-Isopropoxystyrene. Dimerization/dedimerization processes play an important role in the initiation of metathesis using catalysts **1-R$_3$-Cl** but with knowledge of the kinetic and thermodynamic aspects of the equilibria can to some extent be controlled via appropriate manipulation of conditions. With this in mind, we sought to understand the effect of changing substitution at phosphorus on the reactivity of the monomeric forms of **1-R$_3$** with olefin substrates. The reaction we chose to probe this is shown in Scheme 3; it was expected that under pseudo-first-order conditions, reactions of **1-R$_3$** with *o*-isopropoxystyrene yield the known Grubbs/Hoveyda catalyst **II** and a vinylphosphonium phosphonium product.[67] Separate experiments have shown that these vinylphosphonium products are "type IV" substrates[68] that do not undergo metathesis chemistry.[69] Furthermore, under the conditions of these experiments, **II** is not an active metathesis initiator, so the reaction shown in Scheme 3 is effectively irreversible, and its observed

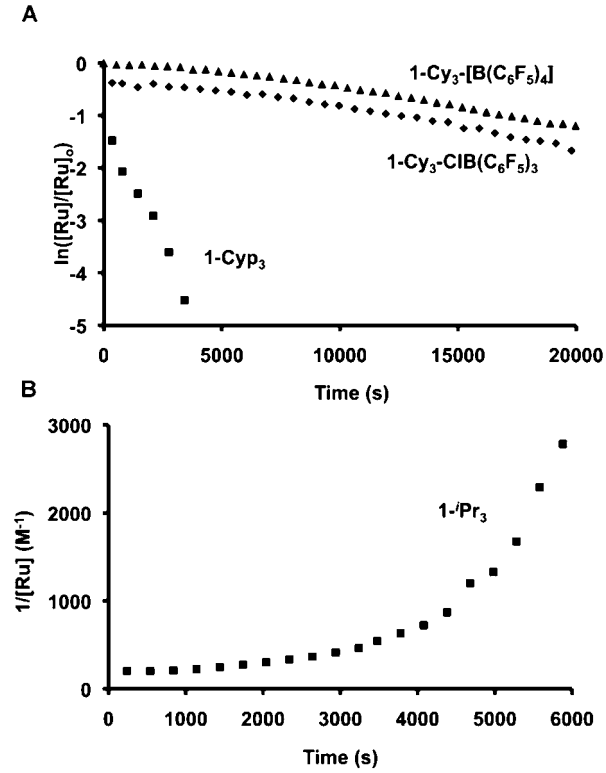

Figure 4. (A) Pseudo-first-order plots for the reactions of **1-Cy$_3$** and **1-Cyp$_3$** with *o*-isopropoxystyrene (1:30) at 243 K. (B) Second-order plot for the reaction of **1-^{i}Pr$_3$** and *o*-isopropoxystyrene (1:1) at 190 K.

rate under pseudo-first-order conditions should allow for extraction of the bimolecular initiation rate of reaction between compounds **1-R$_3$** and the styrene substrate olefin.

Accordingly, reaction of compound **1-Cy$_3$** with 30 equiv of styrene at 243 K proceeds conveniently with a half-life of roughly 1.5 h. Despite the above expectations, the pseudo-first-order plot (Figure 4A, top two curves) displays significant curvature, indicative of an accelerating rate over the initial stages of the reaction.[29] After about 15% conversion, the plot becomes essentially linear; the nature of the anion had no effect on the observed reactivity. On the other hand, the nature of the R group on phosphorus had a significant impact on the rate of the reaction; under the same conditions, compound **1-Cyp$_3$** undergoes the reaction at a much faster rate (Figure 4A, bottom curve), and curvature in the plot is less obviously discernible than for **1-Cy$_3$**, although it is likely present (see below). For **1-^{i}Pr$_3$**, the reaction was too fast to measure its rate under these conditions. Indeed, even under strictly second-order conditions (**1-^{i}Pr$_3$**:*o*-isopropoxystyrene = 1:1) at 190 K, the reaction is very rapid. Here, the second-order plot shown in Figure 4B also exhibits dramatic curvature, with the reaction exhibiting strong rate acceleration as it proceeds. Given the small changes in the cone angles of these PR_3 groups (160°, 167°, 170° for **1-^{i}Pr$_3$**, **1-Cyp$_3$**, and **1-Cy$_3$**, respectively),[42] the differences in reactivity toward the styrene substrate are remarkable and the reactivity of **1-^{i}Pr$_3$** in particular suggests this is a highly potent initiator for olefin metathesis.

(66) Romero, P. E.; Piers, W. E. *J. Am. Chem. Soc.* **2007**, *129*, 1698–1704.

(67) Several of the vinylphosphonium products were isolated and characterized by NMR spectroscopy and ESI mass spectrometry; see Supporting Information.

(68) Chatterjee, A. K.; Choi, T.-L.; Sanders, D. P.; Grubbs, R. H. *J. Am. Chem. Soc.* **2003**, *125*, 11360–11370.

(69) For example, mixing of **1-Cy$_3$** with an excess of the vinyl triisopropylphosphonium cation (both as their BPh_4 salts) shows no reaction over the course of 20 h at room temperature in CD_2Cl_2. Futhermore, no reaction between II and the vinylphosphonium salts was observed even at elevated temperatures for prolonged periods (>24 h).

Scheme 4

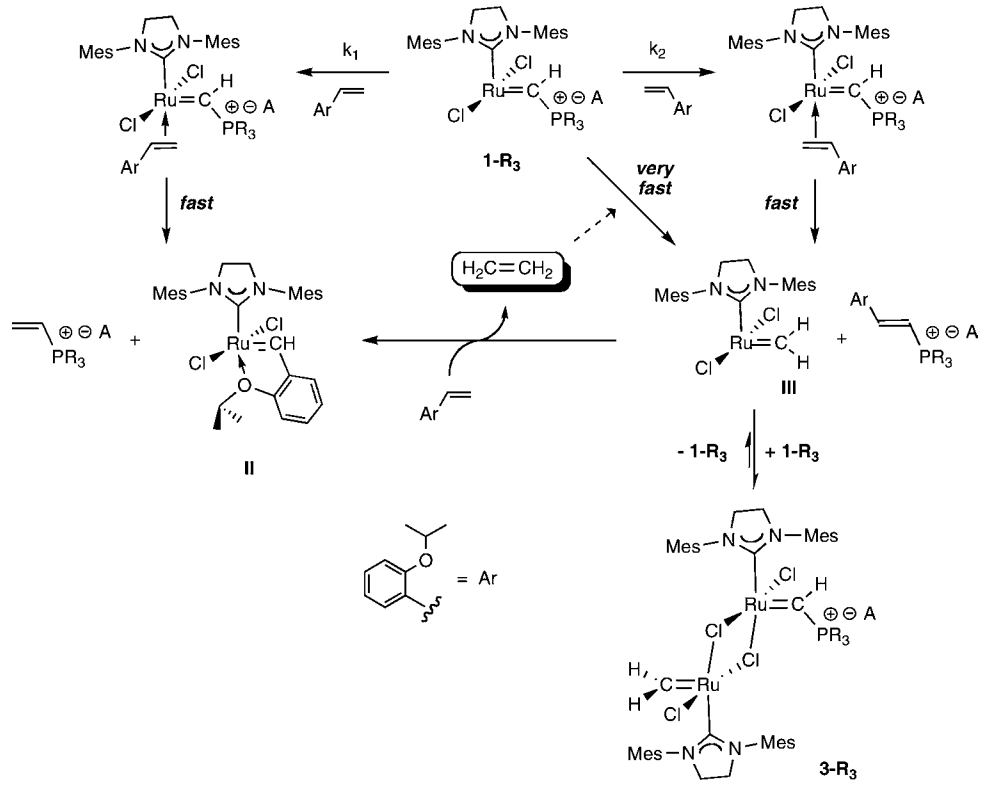

We postulated that the reason behind this behavior stemmed from the availability of two reaction pathways for the styrene substrate to react with compounds **1-PR$_3$**, the expected pathway to generate **II** (Scheme 3) and the opposite regiochemical channel to generate the highly reactive 14-electron methylidene $(H_2IMes)(Cl)_2Ru{=}CH_2$, **III** and an equivalent of the styrenylphosphonium salt as shown in Scheme 4. Intermediate **III**, long-proposed but not observed directly via spectroscopy, would rapidly react with styrene substrate to produce Grubbs−Hoveyda product **II** and generate an equivalent of ethylene. We have shown in some detail that ethylene reacts rapidly with compounds **1-R$_3$** to regenerate **III** and the vinylphosphonium species; thus ethylene has the potential to act as a catalyst for the production of **II** from compounds **1-R$_3$** and the *o*-isopropoxystyrene substrate. Therefore, the curvature observed in the pseudo-first-order and second-order plots discussed above represents the time required to generate sufficient quantities of ethylene (i.e., the ratio of rate constants k_1 and k_2 depicted in Scheme 4) such that the rate-accelerated ethylene catalyzed pathway dominates over the direct reaction of compounds **1-R$_3$** and the *o*-isopropoxystyrene to yield **II**. The generation of trace amounts of ethylene and it's important effect on the elementary steps of metathesis reactions has also been noted recently by Hoveyda and co-workers in a ring-closing metathesis (RCM) reaction using a chiral molybdenum catalyst. Here, production of ethylene is crucial for setting up a degenerate metathesis reaction that establishes Curtin−Hammett conditions and promotes high enantioselectivity.[70] The ethylene is produced from a cross-metathesis reaction of the molybdenum methylidene catalyst (formed after one RCM cycle) and the olefinic substrate for RCM.

Several lines of evidence support the ethylene hypothesis, in our case. First, we observe an 8-fold rate enhancement (and linear pseudo-first-order kinetic behavior) in the reaction of *o*-isopropoxystyrene and **1-Cy$_3$** when a known amount (20%) of ethylene is intentionally added to the reaction (Figure 5). Second, ethylene is detected by ^{1}H NMR spectroscopy ($\delta \sim 5.4$ ppm) in the spectra for all complexes **1-R$_3$**. Third, the styrenylphosphonium byproducts of metathesis by path k_2 can be detected by both electrospray mass spectrometry and NMR spectroscopy. In the ^{31}P NMR spectra, in addition to the signal for $[H_2C{=}C(H)PR_3]^+$, a second, less intense, singlet in the same region of the spectrum is observed for the $[(Ar)HC{=}C(H)PR_3]^+$ species. Only one isomer is observed and analysis of the $^1H\{^{31}P\}$ NMR spectra of the styrenylphosphonium salt produced in the reaction involving **1-^{i}Pr$_3$** suggests that it is the *E*-isomer as shown, on the basis of the large $^3J_{HH}$ coupling constant of $\sim$ 18 Hz. To the extent that the ratio of vinyl to styrenylphosphonium reflects the ratio of k_1 to k_2, these ratios (as determined by ^{31}P NMR spectroscopy and graphically illustrated in Figure 6) are influenced strongly by the size of the PR_3 group. When the alkyl group is large, as in **1-Cy$_3$**, the amounts of this

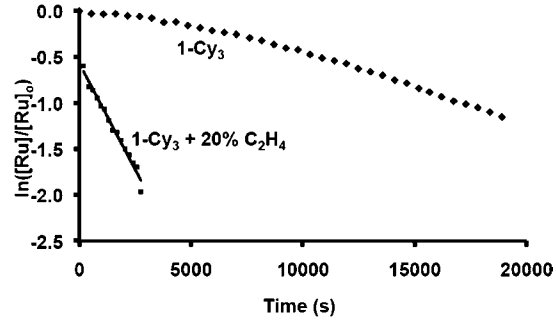

Figure 5. Ethylene-induced rate acceleration in the reaction of **1-Cy$_3$** with 30 equiv of *o*-isopropoxystyrene at 243 K.

(70) Meek, S. J.; Malcolmson, S. J.; Li, B.; Schrock, R. R.; Hoveyda, A. H. *J. Am. Chem. Soc.* **2009**, *131*, 16407–16409.
(71) Ulman, M.; Grubbs, R. H. *Organometallics* **1998**, *17*, 2484–2489.

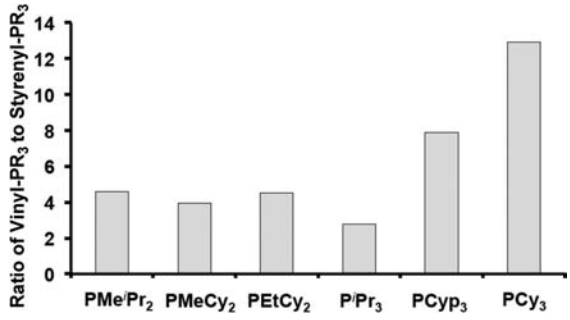

Figure 6. Ratio of the vinylphosphonium salt to the styrenylphosphonium salt for the different catalysts **1-R$_3$** (R$_3$ = Cy$_3$, Cyp$_3$, ^{i}Pr$_3$, EtCy$_2$, Et^{i}Pr$_2$, MeCy$_2$, Me^{i}Pr$_2$).

styrenylphosphonium salt are small, but the proportion increases as the phosphonium group becomes smaller until k_2 is quite competitive with k_1 for the **1-Cyp$_3$** and **1-^{i}Pr$_3$** derivatives.

The mixed phosphonium alkylidenes **1-EtCy$_2$**, **1-Et^{i}Pr$_2$**, **1-MeCy$_2$**, and **1-Me^{i}Pr$_2$** also produce 20−50% of the styrenylphosphonium byproduct, but the situation is somewhat more complex for these initiators in that the reactive methylidene species **III** is trapped by **1-R$_3$** in dimers **3-R$_3$**; this provides good evidence for the involvement of **III** in this chemistry as depicted in Scheme 4. These compounds are presumably related structurally to the dimers **(1-R$_3$)$_2$** discussed above but exhibit more complicated ^{1}H NMR spectra due to their asymmetry. Most informative is the alkylidene region of the spectra, in which two new signals appear in a 1:2 ratio at $\delta \sim 20$ ppm ($^2J_{HP} = 43$ Hz) and $\delta \sim 18$ ppm (singlet) assignable to the phosphonium alkylidene and methylidene portions of the **3-R$_3$** dimer, respectively. Indeed, enriched solutions of binuclear phosphonium alkylidenes **3-R$_3$** can be generated independently via reaction of the corresponding **1-R$_3$** with 0.5 equiv of ethylene.[51] Under the conditions of these experiments, dimers **3-R$_3$**, when observed, eventually react with the excess *o*-isopropoxystyrene present to generate the final product **II**. Attempts to isolate these compounds were unsuccessful; they are not stable at temperatures above 243 K and readily dissociate into **III** and **1-R$_3$**.

Concluding Remarks. The family of phosphonium alkylidenes **1-R$_3$** are among the most rapidly initiating ruthenium-based olefin metathesis catalysts known, but the current study shows that the chemistry associated with the initiation processes is more complex than meets the eye. The role of the substituents at phosphorus is the most important in defining this chemistry, with bulky subsitutents required to stabilize the 14-electron compounds relative to both decomposition pathways and deactivating dimerization pathways. Ultimately, a balance between enough steric bulk to tilt the monomer−dimer equilibrium toward the active monomer and enough steric openness to allow for a low barrier reaction with incoming olefin substrate leads to the most rapidly initiating examples of this family of catalysts. Although **1-Me^{i}Pr$_2$** incorporates the least sterically imposing PR$_3$ group, it exhibits the greatest tendency to dimerize, and so the initiation step becomes dedimerization, a higher barrier process than bimolecular reaction with olefin substrate. All of the unsymmetrically substituted phosphonium alkylidene catalysts suffer from dimerization to some extent.

The trends among the symmetrically substituted catalysts reveal that initiation efficacy is remarkably sensitive to small changes in phosphine cone angle. The reasons for this appear to be 2-fold. First, in order to coordinate substrate olefin in an orientation appropriate for metallacyclobutane formation, the phosphonium alkylidene must rotate from its ground state orientation in which C$_{NHC}$−Ru−C−P are essentially coplanar to one in which the dihedral angle approaches 90° (Scheme 5). This rotation turns on unfavorable steric interactions with the NHC mesityl groups, likely a primary factor in raising the barrier to reaction with olefin substrate. Thus, smaller groups should lead to greater ease in achieving the proper orientation. The second factor involves the ability to shunt the initiation process into the ethylene-mediated reaction channel, which is also favored by smaller substituents on phosphorus. The smaller cone angle of phosphonium alkylidenes allow for k_2 to be more competitive with k_1 (Scheme 4), producing ethylene faster, which in turn accelerates initiation significantly. This "k_2" mode of initiation appears to be general; when **1-^{i}Pr$_3$** is reacted with other terminal olefin substrates such as propene, styrene, and dimethyl diallylmalonate, alkenylphosphonium salts consistent with k_2 reactivity are observed in all cases, indicating that ethylene production is operative for these olefins as well. The extent to which k_2 reactivity occurs appears to track with the steric bulk of the olefin substitutent:[71] for propene, $[(CH_3)CH{=}C(H)P^iPr_3]^+$ forms about 30% of the phosphonium salt complement, whereas for dimethyl diallyl malonate and styrene, the alkenyl phosphonium salts comprised 12% and 5% of the mixture, respectively.[72]

Of the catalysts reported here, then, the triisopropyl derivative **1-^{i}Pr$_3$** strikes the balance between steric bulk and activity most effectively. The P^{i}Pr$_3$ group is large enough to discourage dimerization but small enough to allow the complex to react rapidly with olefin substrates via both k_1 and k_2 pathways. Likely, it is the catalysts' ability to rapidly generate ethylene (see Figure 6) that primarily accounts for its remarkable ability to initiate olefin metathesis at temperatures as low as 190 K. It should be noted that although catalyst **1-^{i}Pr$_3$** is a viable species that can be isolated, its behavior in solution in the absence of a substrate indicates that it decomposes more rapidly ($t_{1/2} \approx$ 1 h at 343 K) than the bulkier **1-Cy$_3$** ($t_{1/2} \approx 2.5$ h at 343 K).[48] We find that it is best to store and use this compound as the chloride-stabilized zwitterion **1-^{i}Pr$_3$-Cl**, prepared as shown in Scheme 1. It is very conveniently activated by B(C$_6$F$_5$)$_3$ and in fact can be activated in the presence of substrate using this methodology. Alternatively, one could contemplate using the somewhat more thermally robust catalysts like **1-Cy$_3$** and boosting their initiation efficiency by intentionally adding ethylene along with substrate. In any case, the representatives of this family of catalysts discussed here exhibit very fast initiating properties that have significant promise for applications

Scheme 5

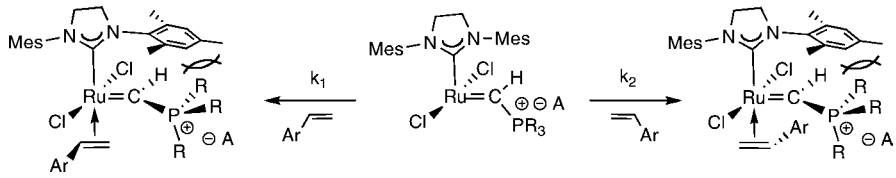

in materials chemistry and fine chemical synthesis due to the mild conditions under which they can initiate metathesis reactions.

Experimental Section

General. Argon-filled VAC dryboxes were used to store air- and moisture-sensitive compounds and for manipulation of air-sensitive materials. Reactions were performed under an argon atmosphere in the drybox. Internal standards 1,3,5-trimethoxybenzene and hexamethyldisiloxane were purchased from Aldrich. $B(C_6F_5)_3$ was purchased from Strem and was sublimed before use. Ethylene was purchased from Matheson and dichloromethane-d_2 was purchased from Cambridge Isotope Laboratories. *o*-Isopropoxystyrene was synthesized by published procedures.[73] All ruthenium-containing starting materials were synthesized by published procedures[29,51,74] or procedures provided in Supporting Information. Where applicable, cooling baths consisting of dry ice/acetone (195 K) were used to maintain low temperature conditions. ^{1}H, ^{31}P{^{1}H} NMR experiments were performed on Bruker 400 MHz spectrometers. Data are given in ppm relative to residual solvent signals for ^{1}H and ^{31}P spectra was referenced to 85% H_3PO_4. Temperature calibration for low temperature NMR experiments was achieved by monitoring the ^{1}H NMR spectrum of pure methanol before and after changing the temperature. For quantitative experiments 16 scans were collected for every spectrum. T_1 measurements were performed on the resonances of interest, and a delay (d_1) of $5*T_1$ between single acquisitions was used, taking as a reference the longest relaxation time. In the case of the initiation kinetics of the ruthenium phosphonium alkylidene complexes, $5*T_1$ corresponded to 6 s. Electrospray ionization mass spectrometry was performed on the Bruker Esquire 3000 (positive mode, 3200V capillary voltage, 7 psi nebulizer, 5.0 L/min dry gas, 573 K dry temperature, 0.10 ms accumulation time, and target mass set between 150−400 *m/z* depending on the phosphonium salt byproduct).

Measurement of Equilibrium Constants for [1-MeCy$_2$]$^+$/([1-MeCy$_2$]$^+$)$_2$. The compound was generated in CD_2Cl_2 containing 0.0062 M $Me_3SiOSiMe_3$ as an internal standard. The temperature in the NMR probe was calibrated using a methanol thermometer. The integrations of the H_2IMes NCH_2CH_2N backbone protons were used in the analysis, since they are distinct and do not overlap with each other or with other peaks. The equilibrium constant K (= $[\text{dimer}]_{eq}/[\text{monomer}]^2_{eq}$) was then determined in the temperature range 295−245 K, in intervals of ca. 5 K. At the lower temperatures, the sample was given 1 h to allow it to fully equilibrate before K was measured.

Measurement of Equilibration and of Equilibrium Constants for [1-EtCy$_2$]/([1-EtCy$_2$])$_2$. The compound was generated at room temperature in CD_2Cl_2 containing 0.0062 M $Me_3SiOSiMe_3$ as an internal standard, after which the sample was quickly immersed in a dry ice/acetone (−78 °C) bath. The temperature in the NMR probe was calibrated using a methanol thermometer, and the NMR tube was quickly transferred from the dry ice/acetone bath to the precooled NMR probe. Concentrations of monomer and dimer were followed over time until equilibrium was attained (except at 207 and 213 K, for which equilibrium was not attained after >14 h). The integrations of the alkylidene (Ru=C*H*) protons were used in the analysis. K was determined after equilibriation, in the temperature range 225−260 K in intervals of ca. 7 K.

Reaction of [1-EtCy$_2$]/([1-EtCy$_2$])$_2$ Mixture with Excess Ethene at 225 K. The compound was generated at room temperature in a J-Young tube in CD_2Cl_2 containing 0.0062 M $Me_3SiOSiMe_3$ as an internal standard, after which the sample was quickly immersed in a dry ice/acetone (−78 °C) bath. The temperature in the NMR probe was calibrated to 225 K using a methanol thermometer, and the NMR tube was quickly transferred from the dry ice/acetone bath to the precooled NMR probe. Concentrations of monomer and dimer were followed over time as described above. After equilibration, the sample was quickly reimmersed in a dry ice/acetone bath, and three freeze−pump−thaw cycles were performed, keeping the temperature at or below −78 °C. An excess (6 and 11 equiv relative to $[\text{Ru}]_{total}$) of ethene was transferred into the tube at −196 °C, after which the tube was thawed at −78 °C and carefully shaken at this temperature. The tube was reinserted into the NMR probe at 225 K, and concentrations of monomer (= 0) and dimer were followed over time as described above.

Reaction of [1-MeCy$_2$]/([1-MeCy$_2$])$_2$ Mixture with Excess Ethene. The compound was generated at room temperature in a J-Young tube in CD_2Cl_2 containing 0.0062 M $Me_3SiOSiMe_3$ as an internal standard. Three freeze−pump−thaw cycles were performed, and the NMR tube was transferred to the NMR probe at 245 K and allowed to equilibrate for 1 h to obtain a ca. 20:1 dimer/monomer mixture. The tube was taken out of the probe, quickly immersed in a dry ice/acetone bath, and an excess (ca. 10 equiv) of ethene was added to the tube as described above. The temperature in the NMR probe was calibrated using a methanol thermometer. The tube was reinserted into the NMR probe, and concentrations of monomer (= 0) and dimer were followed over time as described above. This analysis was performed at four temperatures in the range 235−254 K.

Generation of II from 1-R$_3$-A (30 equiv of *o*-isopropoxystyrene; R$_3$ = Cy$_3$, Cyp$_3$; A = ClB(C$_6$F$_5$)$_3$, B(C$_6$F$_5$)$_4$). $(H_2IMes)(Cl_3)Ru{=}C(H)PR_3$ (6−7 mg, 0.0083 mmol, R = Cy, Cyp) and $B(C_6F_5)_3$ (5 mg, 0.0098 mmol) or $[(H_2IMes)(Cl_2)Ru{=}C(H)PCy_3]^+[B(C_6F_5)_4]^-$ (12 mg, 0.0083 mmol) were charged into an NMR tube along with 0.4 mL of CD_2Cl_2. In a gastight syringe, 200 μL of a stock solution containing *o*-isopropoxystyrene (41 mg, 0.250 mmol) and 1,3,5-trimethoxybenzene internal standard (2.8 mg, 0.017 mmol) was added. The NMR tube was placed in an acetone/dry ice bath for transporting to the precooled NMR probe (243 K) where the stock solution was added at (195 K) before insertion into the probe. The reaction progress was monitored by both ^{1}H and ^{31}P{^{1}H} NMR spectroscopy through cycling experiments, at various intervals (depending on the half-life of the conversion), until essentially all of the starting material catalyst was converted to **II** (δ ∼16 ppm). Integration of the starting complex alkylidene peak (δ ∼18 ppm) against the internal standard (δ = 6.1 ppm) was used for the first-order treatment of the data. ^{31}P{^{1}H} NMR of **1-Cy$_3$** phosphonium byproduct (CD_2Cl_2, 161.8 MHz, 238 K): δ 28.22 ($[(Ar)HC{=}C(H)PCy_3]^+[B(C_6F_5)_4]^-$), 27.41 ($[H_2C{=}C(H)PCy_3]^+[B(C_6F_5)_4]^-$); δ 28.15 ($[(Ar)HC{=}C(H)PCy_3]^+[ClB(C_6F_5)_3]^-$), 27.34 ($[H_2C{=}C(H)PCy_3]^+[ClB(C_6F_5)_3]^-$). ESI MS of **1-Cy$_3$** phosphonium byproduct $C_{20}H_{36}P^+$: 307 *m/z* ($[H_2C{=}C(H)PCy_3]^+$); $C_{29}H_{46}OP^+$: 441 *m/z* ($[(Ar)HC{=}C(H)PCy_3]^+$); $C_{18}F_{15}BCl^-$: 547 *m/z*; $C_{24}F_{20}B^-$: 679 *m/z*. ^{31}P{^{1}H} NMR of **1-Cyp$_3$** phosphonium byproduct (CD_2Cl_2, 161.8 MHz, 238 K): δ 36.48 ($[(Ar)HC{=}C(H)PCyp_3]^+[ClB(C_6F_5)_3]^-$), 35.98 ($[H_2C{=}C(H)PCyp_3]^+[ClB(C_6F_5)_3]^-$). ESI MS of **1-Cyp$_3$** phosphonium byproduct $C_{17}H_{30}P^+$: 265 *m/z* ($[H_2C{=}C(H)PCyp_3]^+$); $C_{26}H_{40}OP^+$: 399 *m/z* ($[(Ar)HC{=}C(H)PCyp_3]^+$); $C_{18}F_{15}BCl^-$: 547 *m/z*.

Generation of II from 1-R$_3$ (1 equiv of *o*-isopropoxystyrene; R$_3$ = ^{i}Pr$_3$, EtCy$_2$, Et^{i}Pr$_2$, MeCy$_2$, Me^{i}Pr$_2$). $(H_2IMes)(Cl_3)Ru{=}C(H)PR_3$ (6−7 mg, 0.0083 mmol, R_3 = ^{i}Pr$_3$, EtCy$_2$, MeCy$_2$, Me^{i}Pr$_2$) and $B(C_6F_5)_3$ (5 mg, 0.0098 mmol) were charged into an NMR tube along with 0.4 mL of CD_2Cl_2. In a gastight syringe 200 μL of a stock solution containing *o*-isopropoxystyrene (1.3 mg, 0.0083 mmol) and 1,3,5-trimethoxybenzene internal

(72) It is not clear why the *o*-isopropoxystyrene gives 35% of the stryrenylphosphonium salt, but the donor properties of the *o*-isopropyl group may play a role in this observation directing the OR group towards the R_3P^+ moiety.

(73) Krause, J. O.; Nuyken, O.; Wurst, K.; Buchmeiser, M. R. *Chem. Eur. J.* **2004**, *10*, 777–784.

(74) Dubberley, S. R.; Romero, P. E.; Piers, W. E.; McDonald, R.; Parvez, M. *Inorg. Chim. Acta* **2006**, *359*, 2658–2664.

standard (2.8 mg, 0.017 mmol) was added. The NMR tube was placed in an acetone/dry ice bath for transport to the precooled NMR probe (190 K) where the stock solution was added at 195 K before inserting into the probe. The reaction progress was monitored by both ^{1}H and ^{31}P{^{1}H} NMR spectroscopy through cycling experiments, at various intervals (depending on the half-life of the conversion), until all of the starting material catalyst was converted to **II** ($\delta \sim$16 ppm). Integration of the starting complex alkylidene peak ($\delta \sim$18 ppm) against the internal standard ($\delta = 6.1$ ppm) was used for the second-order treatments of the data obtained with **1-*i*Pr$_3$** and **1-EtCy$_2$**. Integration of **(1-MeCy$_2$)$_2$** or **(1-Me*i*Pr$_2$)$_2$** alkylidene peaks (19.87, 19.65 ppm, respectively; as all **1-MeCy$_2$** and **1-Me*i*Pr$_2$** were converted to **II** within 5 min of mixing) was used against internal standard ($\delta = 6.1$ ppm) to show that the dimer to monomer equilibrium is extremely slow at 190 K and that the dimers are inert to metathesis with *o*-isopropoxystyrene at this temperature. *1-Et*^{i}*Pr$_2$* was difficult to fit to a second-order plot as the monomer/dimer equilibrium was in operation at this temperature. ^{31}P{^{1}H} NMR of phosphonium byproduct (CD_2Cl_2, 161.8 MHz, 181 K): δ 38.35 ([(Ar)HC═C(H)*P*^{i}Pr$_3$]$^+$[ClB(C$_6$F$_5$)$_3$]$^-$), 38.10 ([H$_2$C═C(H)*P*^{i}Pr$_3$]$^+$[ClB(C$_6$F$_5$)$_3$]$^-$). ESI MS of **1-*i*Pr$_3$** phosphonium byproduct $C_{11}H_{24}P^+$: 187 *m/z* ([H$_2$C═C(H)*P*^{i}Pr$_3$]$^+$); $C_{20}H_{34}OP^+$: 321 *m/z* ([(Ar)HC═C(H)*P*^{i}Pr$_3$]$^+$); $C_{18}F_{15}BCl^-$: 547 *m/z*. ^{31}P{^{1}H} NMR of **1-EtCy$_2$** phosphonium byproduct (CD_2Cl_2, 161.8 MHz, 181 K): δ 31.15 ([(Ar)HC═C(H)*P*EtCy$_2$]$^+$[ClB(C$_6$F$_5$)$_3$]$^-$), 30.82 ([H$_2$C═C(H)-*P*EtCy$_2$]$^+$[ClB(C$_6$F$_5$)$_3$]$^-$). ESI MS of **1-EtCy$_2$** phosphonium byproduct $C_{16}H_{30}P^+$: 253 *m/z* ([H$_2$C═C(H)*P*EtCy$_2$]$^+$); $C_{25}H_{40}OP^+$: 387 *m/z* ([(Ar)HC═C(H)*P*EtCy$_2$]$^+$); $C_{18}F_{15}BCl^-$: 547 *m/z*. ^{31}P{^{1}H} NMR of **1-Et*i*Pr$_2$** phosphonium byproduct (CD_2Cl_2, 161.8 MHz, 181 K): δ 38.32 ([(Ar)HC═C(H)*P*Et^{i}Pr$_2$]$^+$[ClB(C$_6$F$_5$)$_3$]$^-$), 38.23 ([H$_2$C═C(H)-*P*Et^{i}Pr$_2$]$^+$[ClB(C$_6$F$_5$)$_3$]$^-$). ESI MS of **1-Et*i*Pr$_2$** phosphonium byproduct $C_{10}H_{22}P^+$: 173 *m/z* ([H$_2$C═C(H)*P*Et^{i}Pr$_2$]$^+$); $C_{19}H_{32}OP^+$: 307 *m/z* ([(Ar)HC═C(H)*P*Et^{i}Pr$_2$]$^+$); $C_{18}F_{15}BCl^-$: 547 *m/z*. ^{31}P{^{1}H} NMR of **1-MeCy$_2$** phosphonium byproduct (CD_2Cl_2, 161.8 MHz, 181 K): δ 32.90 ([(Ar)HC═C(H)*P*MeCy$_2$]$^+$[ClB(C$_6$F$_5$)$_3$]$^-$), 33.03 ([H$_2$C═C(H)-*P*MeCy$_2$]$^+$[ClB(C$_6$F$_5$)$_3$]$^-$). ESI MS of **1-MeCy$_2$** phosphonium byproduct $C_{15}H_{28}P^+$: 239 *m/z* ([H$_2$C═C(H)*P*MeCy$_2$]$^+$); $C_{24}H_{38}OP^+$: 373 *m/z* ([(Ar)HC═C(H)*P*MeCy$_2$]$^+$); $C_{18}F_{15}BCl^-$: 547 *m/z*. ^{31}P{^{1}H} NMR of **1-Me*i*Pr$_2$** phosphonium byproduct (CD_2Cl_2, 161.8 MHz, 181 K): δ 40.66 ([(Ar)HC═C(H)*P*Me^{i}Pr$_2$]$^+$[ClB(C$_6$F$_5$)$_3$]$^-$), 40.95 ([H$_2$C═C(H)-*P*Me^{i}Pr$_2$]$^+$[ClB(C$_6$F$_5$)$_3$]$^-$). ESI MS of **1-Me*i*Pr$_2$**phosphonium byproduct $C_9H_{20}P^+$: 159 *m/z* ([H$_2$C═C(H)*P*Me^{i}Pr$_2$]$^+$); $C_{18}H_{30}OP^+$: 293 *m/z* ([(Ar)HC═C(H)*P*Me^{i}Pr$_2$]$^+$); $C_{18}F_{15}BCl^-$: 547 *m/z*.

Generation of II from 1-Cy$_3$-B(C$_6$F$_5$)$_4$ (30 equiv of *o*-isopropoxystyrene, 0.20 equiv of ethylene). [(H$_2$IMes)(Cl$_2$)Ru═C(H)PCy$_3$]$^+$[B(C$_6$F$_5$)$_4$]$^-$ (12 mg, 0.0083 mmol) was charged into an NMR tube along with 0.4 mL of CD_2Cl_2. In a gastight syringe 200 μL of a stock solution containing *o*-isopropoxystyrene (41 mg, 0.250 mmol) and 1,3,5-trimethoxybenzene internal standard (2.8 mg, 0.017 mmol) was added. In a separate gastight syringe 50 μL of ethylene (0.0017 mmol) was added. The NMR tube was placed in an acetone/dry ice bath for transporting to the precooled NMR probe (243 K) where the stock solution and ethylene gas were added (through NMR septum) at 195 K before inserting into the probe. The reaction progress was monitored by both ^{1}H and ^{31}P{^{1}H} NMR through cycling experiments, at various intervals (depending on the half-life of the conversion), until essentially all of the starting material catalyst was converted to **II** ($\delta \sim$16 ppm). Integration of the starting complex alkylidene peak ($\delta \sim$18 ppm) against the internal standard ($\delta = 6.1$ ppm) was used for the pseudo-first-order treatment of the data. ^{31}P{^{1}H} NMR of **1-Cy$_3$** phosphonium byproduct (CD_2Cl_2, 161.8 MHz, 238 K): δ 27.34 ([H$_2$C═C(H)*P*Cy$_3$]$^+$[B(C$_6$F$_5$)$_4$]$^-$), no styrenyl phosphonium salt was observed.

Acknowledgment. Funding was provided by NSERC of Canada in the form of a Discovery Grant to W.E.P. and a CGS-D scholarship for E.M.L. The Alberta Ingenuity Fund is thanked for a Studentship to E.F.vdE. Materia Inc. of Pasadena generously provided Grubbs generation 2 catalysts.

Supporting Information Available: Detailed syntheses of catalysts **1-R$_3$** (R$_3$ = Cyp$_3$, EtCy$_2$, MeCy$_2$, Et*i*Pr$_2$, Me*i*Pr$_2$), characterization of [H$_2$C═C(H)PCy$_3$]$^+$ and [(Ar)HC═C(H)PCy$_3$]$^+$, reaction of **1-MeCy$_2$** and **1-Me*i*Pr$_2$** with isopropoxystyrene, derivation of eq 1, and crystallographic data for **1-MeCy$_2$-Cl**, and **1-Me*i*Pr$_2$-Cl** (in CIF format). This material is available free of charge via the Internet at http://pubs.acs.org.

JA910112M